

RRAM-Based Bio-Inspired Circuits for Mobile Epileptic Correlation Extraction and Seizure Prediction

Hao Wang¹, Lingfeng Zhang¹, Erjia Xiao¹, Xin Wang¹, Zhongrui Wang^{2†}, Renjing Xu^{1†}
 The Hong Kong University of Science and Technology(Guangzhou)¹, The University of Hong Kong²
 renjingxu@hkust-gz.edu.cn, zrwang@eee.hku.hk

Abstract

Non-invasive mobile electroencephalography (EEG) acquisition systems have been utilized for long-term monitoring of seizures, yet they suffer from limited battery life. Resistive random access memory (RRAM) is widely used in computing-in-memory(CIM) systems, which offers an ideal platform for reducing the computational energy consumption of seizure prediction algorithms, potentially solving the endurance issues of mobile EEG systems. To address this challenge, inspired by neuronal mechanisms, we propose a RRAM-based bio-inspired circuit system for correlation feature extraction and seizure prediction. This system achieves a high average sensitivity of 91.2% and a low false positive rate per hour (FPR/h) of 0.11 on the CHB-MIT seizure dataset. The chip under simulation demonstrates an area of approximately 0.83 mm² and a latency of 62.2 μ s. Power consumption is recorded at 24.4 mW during the feature extraction phase and 19.01 mW in the seizure prediction phase, with a cumulative energy consumption of 1.515 μ J for a 3-second window data processing, predicting 29.2 minutes ahead. This method exhibits an 81.3% reduction in computational energy relative to the most efficient existing seizure prediction approaches, establishing a new benchmark for energy efficiency.

Keywords

Seizure Detection, EEG, RRAM, Correlation Extraction, Memristor

1 Introduction

Seizure disorders are widely predicted and analyzed using multi-channel electroencephalography (EEG). However, traditional clinical EEG acquisition relies on large-scale hardware systems, which have limited portability and affordability[1]. To address this challenge, new noninvasive mobile EEG acquisition systems have been developed over the last two decades. However, most mobile EEG systems with built-in wireless/bluetooth data transmission modules and seizure detection algorithms fall short in terms of battery life[2].

Traditional seizure detection and prediction algorithms require a complex feature extraction process but support lightweight learning models such as Support Vector Machines (SVM), k-Nearest Neighbors (kNN), and Random Forest (RF) classifiers[3]. Recently, deep learning methods have been employed for seizure prediction, eliminating the need for complex feature extraction processes. Instead, the network directly undertakes feature analysis and seizure predicting. However, these methods consume significant computational resources[4].

RRAM has been leveraged to enhance computing efficiency through its in-memory computing capabilities[5]. Although RRAM-based seizure prediction has successfully reduced the computational energy consumption of deep learning methods, it has not yet been explored for traditional approaches, which combine physical

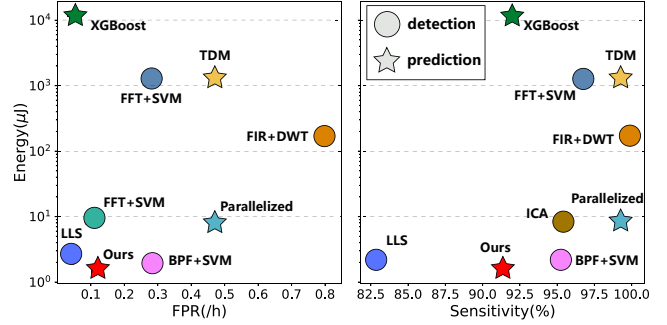


Figure 1: Comparison diagram.

feature extraction with simple models. Correlation is one of the commonly used EEG features[6]. Phase-change memory (PCM)[7] and second-order memristors[8] have been utilized in the study of data correlations.

To minimize the computational energy consumption of seizure detection algorithms, inspired by neuronal correlations, we build a RRAM-Based circuit system for the extraction of EEG correlation features, along with an on-chip neural network system to predict the seizure. Fig. 1 illustrates a comparative analysis between our work and related studies. Our method significantly reduces the computational complexity of the EEG prediction algorithm while ensuring high predictive performance. Our specific contributions are as follows:

- **RRAM-Based Correlation Extraction:** We initially proposed RRAM-based circuits for extracting EEG correlation features and successfully utilized them for seizure prediction.
- **On-chip Energy-Efficient Algorithm:** We have constructed a system for feature extraction and a two-layer epileptic seizure prediction artificial neural network (ANN) using only two 1T1R arrays, sized 18 \times 18 and 18 \times 2. According to our circuits operational logic, this system achieves the lowest energy consumption(1.515 μ J) for current seizure prediction tasks on the CHB-MIT epilepsy dataset, while maintaining high predictive performance.
- **Operational Logic for Specialized Application:** We have developed specialized system operational logic for seizure prediction, which includes unique EEG signal encoding methods, chip architecture reuse strategies, and DAC-less ANN network hardware mapping rules.

2 Background and Related Works

This section begins with an overview of studies on epilepsy algorithms. Then, the discussion turns to the application of memristors in analyzing epilepsy data.

2.1 Seizure Algorithms

Traditional seizure prediction algorithms typically necessitate intricate feature extraction from EEG signals. Techniques commonly

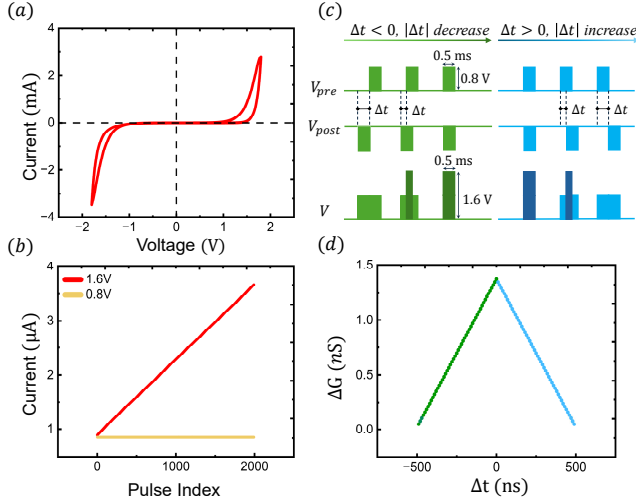


Figure 2: RRAM Model Simulation Diagram. (a) Graph of the current through the memristor versus the voltage difference across its terminals. (b) Relationship between the current through the memristor and the number of pulses, upon inputting 2000 pulses of 1.6V, 500ns, and 0.8V, 500ns. (c) Diagram of the simulation logic used for (d). (d) Graph showing the relationship between pulse overlap ($|\Delta t|$) and the rate of change in conductance (ΔG).

utilized encompass correlation analysis [6], wavelet transform [9], fast Fourier transform (FFT) [10], and least squares parameter estimators [11]. Following this feature extraction, simple learning models, such as support vector machines (SVM), are employed to predict seizures based on the extracted features. In traditional algorithms, the feature extraction process represents the most computationally demanding component.

Recently, the deep learning algorithms, specifically Convolutional Neural Networks (CNN) and Recurrent Neural Networks (RNN), has garnered significant attention in seizure prediction tasks due to their ability to perform feature extraction without complex algorithms. Notable contributions include Hisham Daoud et al.[12], who employed CNNs for EEG feature extraction and RNNs for seizure prediction, achieving a high sensitivity of 99.6% and a low FPR/h of 0.004 on the CHB-MIT dataset, with predictions made up to one hour in advance. Ranjan Jana et al.[13] utilized CNNs for both feature extraction and prediction on the CHB-MIT dataset, optimizing the number of channels from 22 to 6, resulting in a sensitivity of 97.83% and 0.0764 FPR/h, albeit with a prediction window of only 10 minutes.

2.2 Memristors and Epilepsy Analysis

Memristors have been explored in the study of epilepsy-related research. Zhengwu Liu et al.[14] utilized memristor arrays for filtering and recognizing epileptic signals on the Bonn University dataset, achieving a high recognition accuracy of 93.46%. Corey Lammie et al.[15] were the first to implement a deep learning system for seizure prediction on memristors, achieving a prediction sensitivity of 77.4% on the CHB-MIT dataset. Chenqi Li et al.[5] employed a low-latency parallel CNN architecture to perform prediction tasks on the CHB-MIT and SWEC-ETHZ epilepsy datasets, achieving seizure detection sensitivities of 99.24% and 98.22%, but with FPR/h as high as 0.47 and 0.99. Notably, Abu Sebastian et al.[7] used PCM

for studying the correlation of weather information and image data. Yuting Wu et al.[8] employed Second-Order Memristors for researching neuron correlations. Currently, there has been no work that employs traditional non-volatile RRAM for data correlation analysis and uses it for seizure prediction tasks.

3 System Implementation

This section begins with the principles of RRAM, discussing RRAM-based overlap correlation, and outlines the construction and operational architecture of a chip system for processing 18-channel epilepsy EEG data. The EEG-Extracting section introduces the use of memristors for extracting correlation features, while the EEG-Computing section details the neural network structure for seizure prediction and the logic for on-chip operation.

3.1 Memristor Model

In this work, we utilize RRAM devices to extract spike overlap correlations. We will use the WOx-based memristor model proposed in[16] to construct our model:

$$I = (1 - w)\alpha[1 - \exp(-\beta V)] + w\gamma \sinh(\delta V) \quad (1)$$

$$\frac{dw}{dt} = \lambda \sinh(\eta V) \quad (2)$$

Parameters α , β , γ , δ , λ , η are all positive-valued parameters determined by material properties. τ is the diffusion time constant. Additionally, $0 \leq w \leq 1$, $\alpha = 9 \times 10^{-7}$, $\beta = 4$, $\gamma = 2.8 \times 10^{-7}$, $\delta = 6$, $\lambda = 0.045$, $\eta = 6$.

The team provides a SPICE simulation model[17] for the relevant framework, which has been widely used for RRAM simulations. Using the LTspice software, a simulation system was constructed, yielding the imagery depicted in Fig. 2. Part (a) illustrates the quasi-static I-V, with the memristor threshold approximately at 1V. In part (b), linear memristor programming was conducted using 2000 pulses of 1.6V, 500ns and 0.8V, 500ns, respectively; the graph indicates that the 0.8V pulses nearly do not instigate any change in the memristor. In part (c), V_{pre} and V_{post} are respectively applied to the two ends of the memristor, and the differential voltage V is $V_{pre} - V_{post}$. In the diagram, as the Δt changes, the overlap of the pulses first increases and then decreases. In Part (d), stimuli are applied to the memristor following the protocol established in Part (c). It is observed that the change in memristor conductance (ΔG) is positively correlated with the increase in the area of pulse overlap ($|\Delta t|$). This indicates that within a 500 ns timeframe, a greater overlap area of the pulses signifies a higher correlation between the data from the two channels during this period.

3.2 RRAM-Based overlap correlation

The Pearson Correlation Coefficient (PCC) [18], a widely utilized indicator of linear correlation, quantifies the extent to which two variables are interrelated linearly. It gauges how variations in one variable align with changes in another. This relationship is mathematically expressed as:

$$PCC(x_1, x_2) = \frac{\sum_{n=1}^N (x_{1,n} - \bar{x}_1)(x_{2,n} - \bar{x}_2)}{\sqrt{\sum_{n=1}^N (x_{1,n} - \bar{x}_1)^2 \sum_{n=1}^N (x_{2,n} - \bar{x}_2)^2}} \quad (3)$$

Specifically, N is the number of samples. x_1 and x_2 represent the series being analyzed, with \bar{x}_1 and \bar{x}_2 being their respective means. PCC can vary from -1 , indicating a perfect negative linear

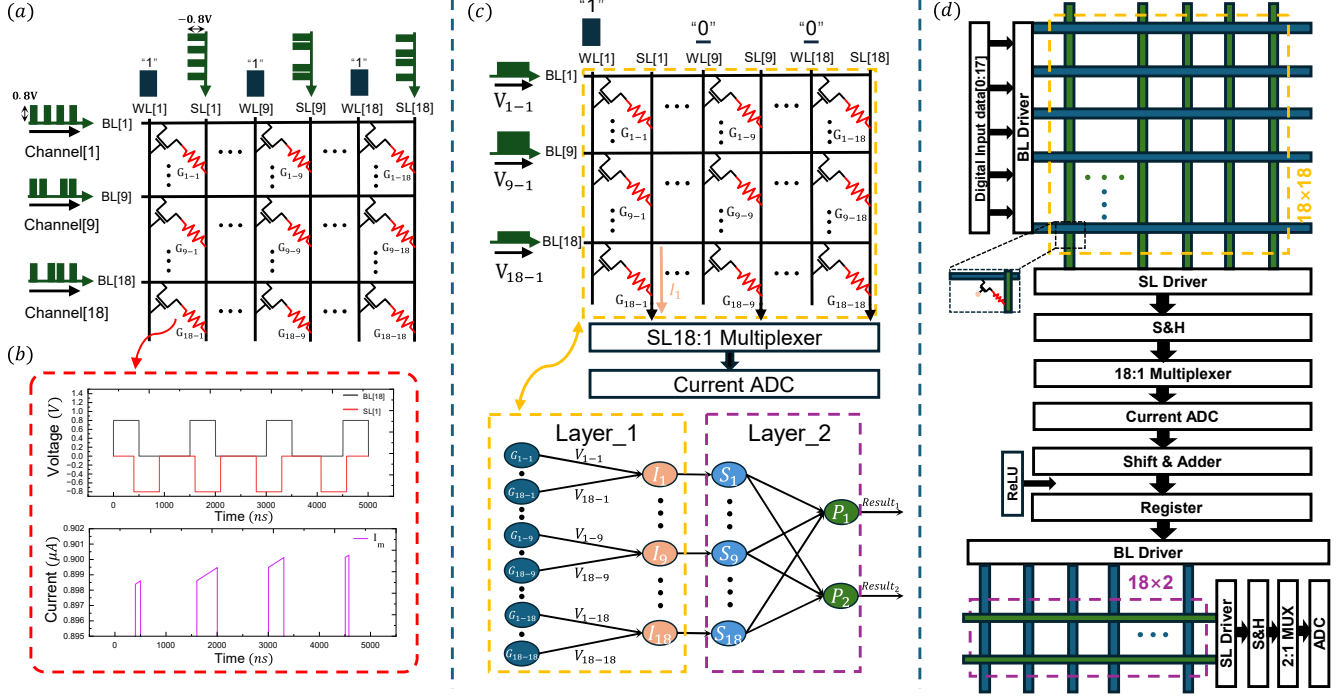


Figure 3: EEG Circuit and System Logic. (a) EEG-Extracting Circuit and Logic. (b) Simulation partial results of the EEG-Extracting phase using RRAM (G_{18-1}) in LTspice. (c) Schematic of the ANN and circuit logic of the first layer network. (d) On-chip EEG-Computing system

relationship, to +1, signifying a perfect positive linear relationship. Synaptic connection strength can be estimated by evaluating the effect of the discharge of a given neuron on the spike probability of another neuron[8]. Inspired by biological relevance, we propose an RRAM-Based Overlap Correlation. Within a 500 ns time window, the memristor emulates a biological synapse where a greater overlap in the pulse signals at both ends of the memristor signifies a larger conductance change (ΔG), indicating stronger signal correlation. Over time, the conductance change (ΔG_k) will accumulate, indicating that the conductance value measured at the end of a period can represent the correlation between the continuous pulse signals at the terminals of the memristor during this interval. This can be represented by the following formula:

$$G_t = \sum_{k=0}^t \Delta G_k + G_0 \quad (4)$$

Here, G_t represents the cumulative value at time t , ΔG_k are incremental changes over time, and G_0 is the initial value. A larger measured conductance value at time t indicates a stronger signal correlation between the two ends over the period from 0 to t .

3.3 EEG-Extracting

Our experiment utilizes the CHB-MIT dataset[19], which contains epileptic EEG data from 18 channels. Consequently, the correlation features comprise 18×18 data. Capitalizing on the overlapping correlation properties of RRAM, we proposed a chip design dedicated to extracting EEG correlation features and predicting seizure, as demonstrated in Fig. 3.

Fig. 3 (a) illustrates the detailed operational logic of an 18×18 array during the EEG-Extracting phase. All WLs are set to '1', fully

activating the transistors, thereby enabling the one-to-one input of EEG data from 18 channels along rows and columns at the BLs and SLs sides, respectively. The BLs are fed with positive pulses of 0.8V, 500ns, while the SLs side receives negative pulses of -0.8V, 500ns. Each memristor sequentially records the cumulative overlap correlation values between pairs of EEG channels. Ultimately, the correlation magnitudes of the 18 EEG channels are mapped to the sizes of the 18×18 conductance values within the array.

Based on the correspondence of channel overlap correlation, we have assigned designations to the memristors, ranging from G_{1-1} to G_{18-18} , totaling 324 identifiers. We conducted a preliminary test of the system using the LTspice software. Fig. 3 (b) presents a partial simulation image of the memristor labeled G_{18-1} . From this, we observe that the change of the memristor conductance value varies with the size of the pulse overlap area, corroborating the characteristics shown in Fig. 2 (b).

3.4 EEG-Computing

Following the EEG-Extracting phase, in pursuit of minimal energy consumption, we explored the use of a two-layer neural network specifically for the task of seizure prediction. The first layer of the network, which is directly implemented on the EEG-Extracting circuits. The second layer is mapped onto the RRAM chip with specific rules.

Fig. 3 (c) presents the neural network model employed for the seizure prediction, and succinctly describes the implementation of the first network layer using the same chip as that utilized for EEG-extracting. Following the EEG-Extracting phase, the memristor conductance values-representing EEG correlations are utilized as inputs for the ANN. Considering the voltage threshold of 1V for

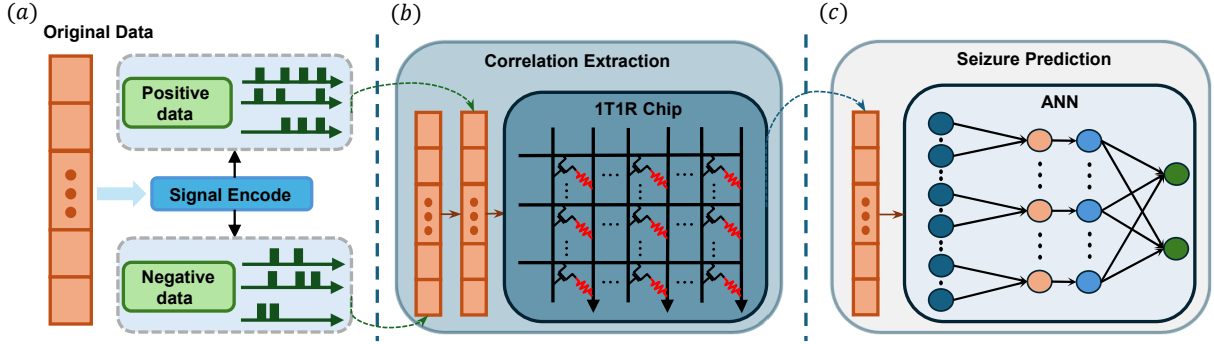


Figure 4: RRAM-Based System Framework. (a) EEG Signal encoding. (b) Correlation Extraction. (c) Seizure Prediction

the memristor, the weights of the first layer of the neural network are trained within a range of 0 to 1. Since the EEG correlations are already stored on-chip, it is only necessary to convert the first layer network weight values into corresponding voltage values and input them sequentially from the BLs side. Subsequently, by employing the multiplexer on the SLs side and the ADC module, the accumulated currents can be read out column by column, completing the computation of the first neural network layer.

Based on the circuits provided by the classic memristor chip[20], we introduce an EEG-Computing circuit for seizure prediction, as illustrated in Fig. 3 (d). To achieve robust computation, the input weights of the first layer network are supplied by digital signals. The output of this network layer is obtained through the logic operation depicted in Fig. 3 (c). Due to the use of digital signals for computations, a Shift&Adder structure is required after the ADC module. A ReLU activation function is employed between the two network layers. The second network layer utilizes standard on-chip RRAM In-Memory Computing execution rules[21]. Mapping the 0-1V voltage weights of the first layer to digital signals can reduce the utilization of Digital-to-Analog Converters (DACs), thereby decreasing chip area and lowering energy consumption. However, this introduces the use of Shift&Adders and incurs increased latency.

4 Evaluation

This section details the implementation and simulation results of a seizure prediction experiment, as shown in Fig. 4. Initially, we describe the data preprocessing steps. This is followed by a discussion on the methods used and the results obtained from the extraction of correlation features. Next, we explore the implementation and outcomes of the seizure prediction task. Finally, we present the energy consumption for the chip system and compare with other studies.

4.1 Experimental preparation

In epilepsy-related analysis tasks, EEG signals can be segmented into three distinct phases: *ictal*, *preictal*, and *interictal*. The ictal samples indicate the occurrence of a seizure at the current moment. In contrast, preictal samples are used to predict the onset of an ictal phase. Interictal samples denote the data recorded between two epileptic seizures, defined as the period at least four hours before and after a seizure event[22]. For seizure detection tasks, a binary classification is performed between the ictal and interictal samples. Meanwhile, for seizure prediction tasks, the classification is between

preictal and interictal samples[5]. Given the subtler differences between the preictal and interictal signals, seizure prediction tasks are more difficult.

Dataset. We employed the CHB-MIT dataset[19] to validate our method. This dataset comprises scalp electroencephalogram (sEEG) data from 23 pediatric patients, encompassing 844 hours of continuous sEEG recordings and 163 seizures. The sEEG signals were captured using 22 electrodes at a sampling rate of 256Hz. Following the criteria established in previous work [22], seizures occurring within 30 minutes of the last seizure were considered as a single seizure. Additionally, patient samples had to include at least two seizures and three hours of interictal period. After selection, 13 patients met our criteria, as detailed in Table 2.

Data Preprocessing. Due to the presence of invalid information in certain channels of the dataset, we selected specific channels for further analysis: 'FP1-F3', 'F3-C3', 'C3-P3', 'P3-O1', 'FP2-F4', 'F4-C4', 'C4-P4', 'P4-O2', 'FP1-F7', 'F7-T7', 'T7-P7', 'P7-O1', 'FP2-F8', 'F8-T8', 'T8-P8', 'P8-O2', 'FZ-CZ', 'CZ-PZ'. These 18 channels were chosen to conduct the experiments. To mitigate the influence of noise, the raw data was filtered to a frequency range of 0-50 Hz[22]. Additionally, the data was segmented into 3-second windows to create samples for analysis. Finally, all memristors must be pre-set to their lowest conductance state.

Signal Encoding. According to the correlation feature extraction rules described in the EEG-Extracting phase, it is necessary to encode epileptic EEG signals. The EEG signals are encoded into continuous pulse signals to preserve as much information as possible. The encoding rules, illustrated in Fig. 5 (a), are proposed as follows: Two voltage thresholds, V_{pth} (Positive threshold) and V_{nth} (Negative threshold), are set. If the EEG signal amplitude exceeds V_{pth} or falls below V_{nth} , a pulse with a voltage amplitude of 0.8V and a width of 40ns is generated. According to these rules, two types of data, Positive data and Negative data, can be obtained.

4.2 Correlation extraction

Following the structure depicted in Fig. 4 (b), after obtaining the Positive data and Negative data, these data sets are fed into the memristor circuit in sequence, starting with the Positive data and then the Negative data. Subsequently, correlation feature extraction is performed on the memristor chip according to the rules outlined in the EEG-Extracting stage. An example of the experimental results is shown in Fig. 5.

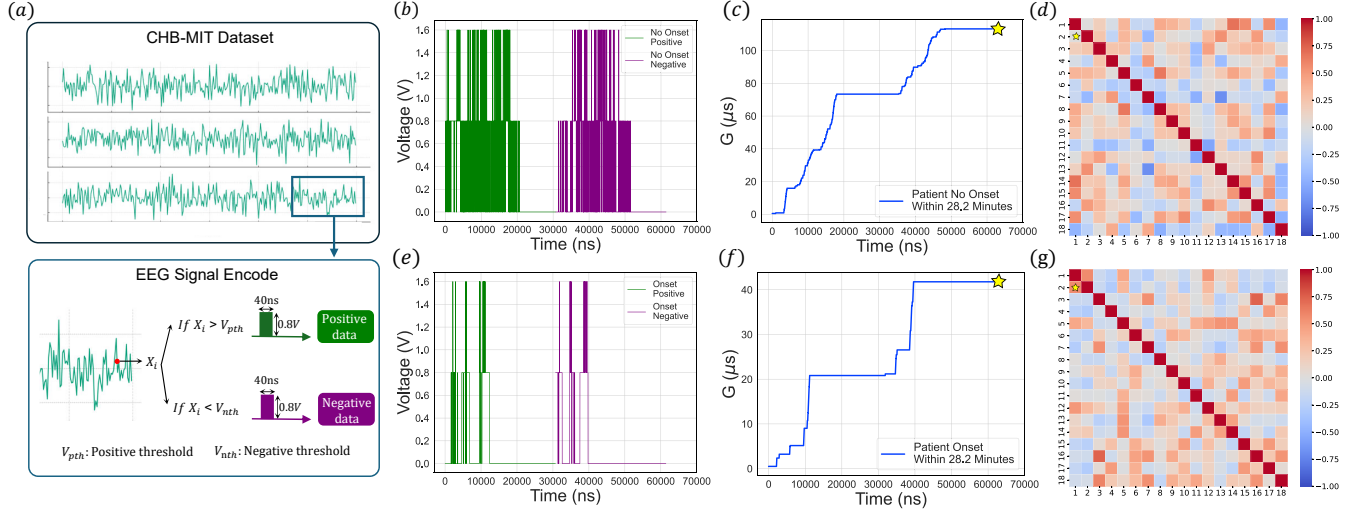


Figure 5: Signal Encoding(a) and Correlation Extraction Example. (b)(c)(d) Predicted as non-disease: (b) shows the voltage difference between Channel-2 and Channel-1 for Patient-1; (c) corresponds to the changes in memristor conductance associated with this voltage difference; (d) displays the correlation map. (e)(f)(g) Predicted as disease: (e) shows the voltage difference between Channel-2 and Channel-1 for Patient-1; (f) corresponds to the changes in memristor conductance associated with this voltage difference; (g) displays the correlation map.

Fig. 5 (a) shows the Positive data represented by dark green blocks and the Negative data represented by purple blocks. Fig. 5 (b) and (c) illustrate the correlation changes between Channel-2 and Channel-1 data when Patient-1 is predicted not to experience a seizure within 28.2 minutes. Fig. 5 (b) depicts the voltage difference between the encoded data of Channel-2 and Channel-1 over time, with the first part representing Positive data and the second part representing Negative data. Fig. 5 (c) shows the conductance values of the corresponding RRAM over time. Finally, Fig. 5 (d) presents the correlation map of Patient-1 when predicted not to experience a seizure within 28.2 minutes. The conductance value at the last time point in Fig. 5 (c) corresponds to the (1, 2) point in Fig. 5 (d), utilizing asterisks as markers. Similarly, Fig. 5 (e) and (f) describe the correlation changes between Channel-2 and Channel-1 data when Patient-1 is predicted to experience a seizure within 28.2 minutes. Fig. 5 (g) presents the correlation map of Patient-1 when predicted to experience a seizure within 28.2 minutes.

4.3 Seizure Prediction

According to the structure depicted in Fig. 4 (c), after extracting an 18×18 correlation feature matrix on-chip, we proceed with the seizure prediction task following the rules of EEG-Computing. The prediction algorithm is an ANN consisting of only two simple layers: the first layer contains 324 weights, and the second layer contains 36 weights. This network is mapped onto the RRAM chip, as shown in Fig. 3 (d).

Based on the criteria previously outlined, seizure prediction was conducted for 13 patients from the CHB-MIT dataset. The details are presented in Table 2. The average lead time for prediction was 29.2 minutes, with an average sensitivity of 91.2%, and FPR/h of 0.11. Comparisons with other tasks are shown in Table 3, indicating that our method maintains high sensitivity and a low FPR/h in seizure prediction tasks. Additionally, there is a trade-off between FPR/h and sensitivity, which must be considered collectively during

task execution. Furthermore, seizure detection and prediction are fundamentally distinct tasks. Therefore, comparisons with seizure detection are provided for reference only.

4.4 Energy Estimation

The core components of our proposed chip architecture (1T1R Chip, Driver, Sample and Hold (S&H), Shift & Adder, Multiplexer (MUX), MUX Decoder) are based on the architecture design and parameters of a physical chip at the 130nm technology node published in[20]. The peripheral circuit components (ReLU, eDRAM Buffer, eDRAM-Tile Bus, Input Register (IR), Output Register (OR)) adopt the system framework and parameters proposed in the most relevant paper[5] at the 22nm technology node, with power calculations performed by referencing the simulation method of MemTorch [30]. Specifically, the ADC component uses an 8-bit, 2 mW power consumption, and 1GS/s sampling speed high-speed low-power ADC[31]. The runtime for the EEG-Extracting stage is 61.44 μs , and the EEG-Computing stage operates at a digital frequency of 1GHz for 836 ns. To estimate the maximum energy consumption, it is assumed that the EEG-Extracting stage continuously emits pulses (maintaining a 1.6V voltage differential on the memristor) and the EEG-Computing stage maintains a voltage of 1V (not affecting the memristor's maximum voltage). The runtime of all modules in each phase is considered to be equal to the maximum runtime.

The results are presented in Table 1, showing a chip area of approximately 0.83 mm², a total execution time for the prediction task of approximately 62.2 μs , power consumption of about 24.4 mW during the EEG-Extracting phase, and about 19.01 mW during the EEG-Computing phase. The total energy consumption for extracting correlation features from epilepsy data over a 3s window and predicting 29.2 minutes in advance is about 1.515 μJ . The core components are responsible for a mere 129.36 nJ of energy consumption, constituting only 8.5% of the total, which suggests significant opportunities for optimization in the peripheral circuits, such as

Table 1: POWER, AREA, LATENCY AND ENERGY CONSUMPTION

Component	Params.	EEG Extracting						EEG Computing						Technology
		Spec.	Area (mm ²)	Power (mW)	Latency (us)	T. Latency ¹ (us)	Energy (nJ)	Spec.	Area (mm ²)	Power (mW)	Latency (us)	T. Latency (us)	Energy (nJ)	
WL Dirver	Number	18	2.90E-04	5.50E-03	2.00E-06	6.14E+01	3.07E-01	20	3.28E-04	5.88E-03	2.00E-06	6.40E-01	3.76E-03	CMOS(130nm)
BL Dirver	Number	18	2.90E-04	5.50E-03	2.00E-06	6.14E+01	3.07E-01	36	5.90E-04	1.05E-02	2.00E-06	6.40E-01	6.72E-03	CMOS(130nm)
SL Dirver	Number	18	2.90E-04	5.50E-03	2.00E-06	6.14E+01	3.07E-01	20	3.28E-04	5.88E-03	2.00E-06	6.40E-01	3.76E-03	CMOS(130nm)
Shift&Adder	Number	-	-	-	-	-	-	1	2.18E-04	1.00E-02	1.90E-04	6.40E-01	6.40E-03	CMOS(130nm)
S&H	Number	-	-	-	-	-	-	40	1.56E-06	4.00E-04	8.33E-04	6.40E-01	2.60E-04	CMOS(130nm)
MUX	Number	-	-	-	-	-	-	2	2.72E-04	7.40E-03	8.00E-06	6.40E-01	4.74E-03	CMOS(130nm)
MUX decoder	Number	-	-	-	-	-	-	2	1.00E-05	1.56E-04	6.00E-04	7.00E-01	1.09E-04	CMOS(130nm)
ADC	Resolution	-	-	-	-	-	-	8 bits	-	-	-	-	-	-
	Number	-	-	-	-	-	-	2	3.00E-03	2.00E+00	1.00E-03	6.40E-01	1.28E+00	CMOS(32nm)
	Sampling Speed	-	-	-	-	-	-	1GS/s	-	-	-	-	-	-
ReLU	Number	-	-	-	-	-	-	1	4.80E-03	1.64E-02	9.80E-02	9.80E-02	3.22E-06	CMOS(22nm)
eDRAM Buffer	Size	2KB	4.72E-03	1.81E+01	1.15E-04	6.14E+01	1.11E+03	2KB	4.72E-03	1.81E+01	1.15E-04	6.40E-01	1.16E+01	CMOS(22nm)
	Bus Width	128	-	-	-	-	-	128	-	-	-	-	-	-
eDRAM Bus	Number	192	4.50E-03	3.50E+00	9.02E-05	6.14E+01	2.15E+02	192	4.50E-03	3.50E+00	9.02E-05	6.40E-01	2.24E+00	CMOS(22nm)
Input Register	Size	1KB	8.10E-01	6.74E-01	8.21E-05	6.14E+01	4.14E+01	1KB	8.10E-01	6.74E-01	8.21E-05	6.40E-01	4.30E-01	CMOS(22nm)
Output Register	Size	-	-	-	-	-	-	512B	8.70E-04	4.18E-01	8.21E-05	6.40E-01	2.67E-01	CMOS(22nm)
Crossbar	Size	18×18	3.24E-06	2.07E+00	6.00E-03	6.14E+01	1.27E+02	18×18	3.60E-06	1.44E+00	6.00E-03	3.80E-02	5.40E-02	RRAM(BEOL)
		18×2	-	-	-	-	-	18×2	-	-	-	-	-	-
Total	-	-	8.20E-01	2.44E+01	-	6.14E+01	1.50E+03	-	8.30E-01	1.90E+01	-	8.36E-01	1.59E+01	-

¹ T.Latency means total latency.

Table 2: PREDICTION RESULTS

Patient	Predicted Time(min)	Sensitivity (%)	FPR(h)
1	28.2	96.2	0.055
2	30	89.1	0.057
3	28.7	88	0.078
6	28.7	83.3	0.184
7	30	94.2	0.146
9	30	88.6	0.18
11	30	89.2	0.1
18	24.2	97.1	0.202
19	30	86.3	0.084
20	30	96.3	0.042
21	30	89.7	0.16
22	30	94.6	0.062
23	30	92.5	0.08
Avg.	29.2	91.2	0.11

Table 3: COMPARISON

Method	Number of Patients	Feature Extraction	Area (mm ²)	Latency (ms)	Power (mw)	Energy (uj)	Sensitivity (%)	FPR/h	Eval. Task(s)
Detection									
APEN,LLS[23]	4	✓	13.47	800	2.8	77.91	92	-	Long Evans rats
BPF,SVM[24]	24	✓	25	2000	0.23	1.83	95.1	0.27	CHB-MIT
FIR,DWT[25]	-	✓	7.59	250	0.674	168.6	100	0.81	EU intracranial
FFT,SVM[26]	24	✓	4.5	710	1.9	1350	96.6	0.28	CHB-MIT
ICA[27]	-	✓	0.4	100	0.0816	8.16	95.24	0.09	Tzu Chi Medical Center
LLS[28]	24	✓	25	2000	0.066	2.03	82.7	0.045	CHB-MIT
Prediction									
XGBoost[29]	7	✓	-	-	2.42	12410	92	0.039	Kaggle
TDM[15]	5	✗	0.1269	1.408	13.3	187	78	7.88	CHB-MIT
Parallelized[15]	5	✗	8.5089	0.011	1700	187	78	7.88	CHB-MIT
TDM[5]	8	✗	31.25	0.445	2790	1240	99.24	0.47	CHB-MIT
Parallelized[5]	8	✗	322.31	0.0011	7200	8.12	99.24	0.47	CHB-MIT
Ours	13	✓	0.83	0.0622	24.4/19.01	1.515	91.2	0.11	CHB-MIT

optoelectronic interconnect technologies. Comparisons with other results are shown in Table 3, demonstrating about 81.3% savings in computational energy compared to the current lowest energy consumption seizure prediction tasks, and even at the estimated maximum energy limit, it remains the lowest among current seizure detection and prediction tasks. This approach can also be extended to other EEG tasks (the number of channels corresponding to array scale).

5 CONCLUSION

This study proposes a chip architecture and operational logic based on RRAM for reducing power consumption in correlation feature extraction and seizure prediction algorithms, enhancing the battery life of non-invasive mobile EEG collection systems. The proposed system achieves a high average sensitivity of 91.2% and a low FPR/h

of 0.11 on the CHB-MIT seizure dataset. The total energy consumption for extracting correlation features from epilepsy data over a 3s window and predicting 29.2 minutes in advance is approximately 1.515 μ J. The proposed method achieves a computational energy saving of about 81.3% compared to the current lowest energy consumption (8.12 μ J) for epileptic seizure prediction tasks. This establishes a new benchmark for the lowest energy consumption. Due to our experiments utilizing the classic characteristics of non-volatile RRAM, such as Long-Term Potentiation (LTP) and threshold effects, this implies the possibility of further implementation on standard RRAM processes. This could facilitate the development of low-power chips designed for EEG correlation feature extraction and seizure prediction. Furthermore, the methodology can be extended to other EEG-related tasks.

References

- [1] Andrea Biondi, Viviana Santoro, Pedro F Viana, Petroula Laiou, Deb K Pal, Elisa Bruno, and Mark P Richardson. Noninvasive mobile eeg as a tool for seizure monitoring and management: A systematic review. *Epilepsia*, 63(5):1041–1063, 2022.
- [2] Elisaveta Sokolov, DH Abdoul Bachir, Foksuna Sakadi, Jennifer Williams, Andre C Vogel, Mike Schaeckermann, Nana Tassiou, Aisatou Kenda Bah, Vidita Khatri, Gladia C Hotan, et al. Tablet-based electroencephalography diagnostics for patients with epilepsy in the west african republic of guinea. *European journal of neurology*, 27(8):1570–1577, 2020.
- [3] Mohammad Khubeb Siddiqui, Ruben Morales-Menendez, Xiaodi Huang, and Nasir Hussain. A review of epileptic seizure detection using machine learning classifiers. *Brain informatics*, 7(1):5, 2020.
- [4] Fatma E Ibrahim, Heba M Emara, Walid El-Shafai, Mohamed Elwekeil, Mohamed Rihan, Ibrahim M Eldokany, Taha E Taha, Adel S El-Fishawy, El-Sayed M El-Rabaie, Essam Abdellatef, et al. Deep-learning-based seizure detection and prediction from electroencephalography signals. *International Journal for Numerical Methods in Biomedical Engineering*, 38(6):e3573, 2022.
- [5] Chenqi Li, Corey Lammie, Xuening Dong, Amirali Amirsoleimani, Mostafa Rahimi Azghadi, and Roman Genov. Seizure detection and prediction by parallel memristive convolutional neural networks. *IEEE Transactions on Biomedical Circuits and Systems*, 16(4):609–625, 2022.
- [6] James R Williamson, Daniel W Bliss, David W Browne, and Jaishree T Narayanan. Seizure prediction using eeg spatiotemporal correlation structure. *Epilepsy & behavior*, 25(2):230–238, 2012.
- [7] Abu Sebastian, Tomas Tuma, Nikolaos Papandreou, Manuel Le Gallo, Lukas Kull, Thomas Parnell, and Evangelos Eleftheriou. Temporal correlation detection using computational phase-change memory. *Nature Communications*, 8(1):1115, 2017.
- [8] Yuting Wu, John Moon, Xiaojian Zhu, and Wei D Lu. Neural functional connectivity reconstruction with second-order memristor network. *Advanced Intelligent Systems*, 3(8):2000276, 2021.
- [9] Yinxia Liu, Weidong Zhou, Qi Yuan, and Shuangshuang Chen. Automatic seizure detection using wavelet transform and svm in long-term intracranial eeg. *IEEE transactions on neural systems and rehabilitation engineering*, 20(6):749–755, 2012.
- [10] Guangyi Chen. Automatic eeg seizure detection using dual-tree complex wavelet-fourier features. *Expert Systems with Applications*, 41(5):2391–2394, 2014.
- [11] Luigi Chisci, Antonio Mavino, Guido Perferi, Marco Sciandrone, Carmelo Anile, Gabriella Colicchio, and Filomena Fuggetta. Real-time epileptic seizure prediction using ar models and support vector machines. *IEEE Transactions on Biomedical Engineering*, 57(5):1124–1132, 2010.
- [12] Hisham Daoud and Magdy A Bayoumi. Efficient epileptic seizure prediction based on deep learning. *IEEE transactions on biomedical circuits and systems*, 13(5):804–813, 2019.
- [13] Ranjan Jana and Imon Mukherjee. Deep learning based efficient epileptic seizure prediction with eeg channel optimization. *Biomedical Signal Processing and Control*, 68:102767, 2021.
- [14] Zhengwu Liu, Jianshi Tang, Bin Gao, Peng Yao, Xinyi Li, Dingkun Liu, Ying Zhou, He Qian, Bo Hong, and Huaqiang Wu. Neural signal analysis with memristor arrays towards high-efficiency brain-machine interfaces. *Nature communications*, 11(1):4234, 2020.
- [15] Corey Lammie, Wei Xiang, and Mostafa Rahimi Azghadi. Towards memristive deep learning systems for real-time mobile epileptic seizure prediction. In *2021 IEEE International Symposium on Circuits and Systems (ISCAS)*, pages 1–5. IEEE, 2021.
- [16] Fuxi Cai, Justin M Correll, Seung Hwan Lee, Yong Lim, Vishishtha Bothra, Zhengya Zhang, Michael P Flynn, and Wei D Lu. A fully integrated reprogrammable memristor-cmos system for efficient multiply-accumulate operations. *Nature electronics*, 2(7):290–299, 2019.
- [17] Ting Chang, Sung-Hyun Jo, Kuk-Hwan Kim, Patrick Sheridan, Sidharth Gaba, and Wei Lu. Synaptic behaviors and modeling of a metal oxide memristive device. *Applied physics A*, 102:857–863, 2011.
- [18] Israel Cohen, Yiteng Huang, Jingdong Chen, Jacob Benesty, Jacob Benesty, Jingdong Chen, Yiteng Huang, and Israel Cohen. Pearson correlation coefficient. *Noise reduction in speech processing*, pages 1–4, 2009.
- [19] Ali Hossam Shoeb. *Application of machine learning to epileptic seizure onset detection and treatment*. PhD thesis, Massachusetts Institute of Technology, 2009.
- [20] Peng Yao, Huaqiang Wu, Bin Gao, Jianshi Tang, Qingtian Zhang, Wenqiang Zhang, Joshua Yang, and He Qian. Fully hardware-implemented memristor convolutional neural network. *Nature*, 577(7792):641–646, 2020.
- [21] Wenbin Zhang, Peng Yao, Bin Gao, Qi Liu, Dong Wu, Qingtian Zhang, Yuankun Li, Qi Qin, Jiaming Li, Zhenhua Zhu, et al. Edge learning using a fully integrated neuro-inspired memristor chip. *Science*, 381(6663):1205–1211, 2023.
- [22] Nhan Duy Truong, Anh Duy Nguyen, Levin Kuhlmann, Mohammad Reza Bonyadi, Jiawei Yang, Samuel Ippolito, and Omid Kavehei. Convolutional neural networks for seizure prediction using intracranial and scalp electroencephalogram. *Neural Networks*, 105:104–111, 2018.
- [23] Wei-Ming Chen, Herming Chiueh, Tsan-Jieh Chen, Chia-Lun Ho, Chi Jeng, Ming-Dou Ker, Chun-Yu Lin, Ya-Chun Huang, Chia-Wei Chou, Tsun-Yuan Fan, et al. A fully integrated 8-channel closed-loop neural-prosthetic cmos soc for real-time epileptic seizure control. *IEEE journal of solid-state circuits*, 49(1):232–247, 2013.
- [24] Muhammad Awais Bin Altaf and Jerald Yoo. A 1.83 μ j/classification, 8-channel, patient-specific epileptic seizure classification soc using a non-linear support vector machine. *IEEE Transactions on Biomedical Circuits and Systems*, 10(1):49–60, 2015.
- [25] Gerard O’Leary, M Reza Pazhouhandeh, Michael Chang, David Groppe, Taufik A Valiante, Naveen Verma, and Roman Genov. A recursive-memory brain-state classifier with 32-channel track-and-zoom δ 2 σ adcs and charge-balanced programmable waveform neurostimulators. In *2018 IEEE International Solid-State Circuits Conference-(ISSCC)*, pages 296–298. IEEE, 2018.
- [26] Shuo-An Huang, Kai-Chieh Chang, Horng-Huei Liou, and Chia-Hsiang Yang. A 1.9-mw svm processor with on-chip active learning for epileptic seizure control. *IEEE Journal of Solid-State Circuits*, 55(2):452–464, 2019.
- [27] Chia-Hsiang Yang, Yi-Hsin Shih, and Herming Chiueh. An 81.6 μ W fastica processor for epileptic seizure detection. *IEEE Transactions on Biomedical Circuits and Systems*, 9(1):60–71, 2014.
- [28] Jerald Yoo, Long Yan, Dina El-Damak, Muhammad Awais Bin Altaf, Ali H Shoeb, and Anantha P Chandrakasan. An 8-channel scalable eeg acquisition soc with patient-specific seizure classification and recording processor. *IEEE journal of solid-state circuits*, 48(1):214–228, 2012.
- [29] Farzad Samie, Sebastian Paul, Lars Bauer, and Jorg Henkel. Highly efficient and accurate seizure prediction on constrained iot devices. In *2018 Design, Automation & Test in Europe Conference & Exhibition (DATE)*, pages 955–960. IEEE, 2018.
- [30] Corey Lammie, Wei Xiang, Bernabé Linares-Barranco, and Mostafa Rahimi Azghadi. Memtorch: An open-source simulation framework for memristive deep learning systems. *Neurocomputing*, 485:124–133, 2022.
- [31] Lukas Kull, Thomas Toifl, Martin Schmatz, Pier Andrea Francese, Christian Menolfi, Matthias Braendli, Marcel Kossel, Thomas Morf, Toke Meyer Andersen, and Yusuf Leblebici. A 3.1 mw 8b 1.2 gs/s single-channel asynchronous sar adc with alternate comparators for enhanced speed in 32 nm digital soi cmos. *IEEE Journal of Solid-State Circuits*, 48(12):3049–3058, 2013.